Biogeosciences Discuss., 10, 11155–11179, 2013
www.biogeosciences-discuss.net/10/11155/2013/
doi:10.5194/bgd-10-11155-2013

Biogeosciences Discussions
Open Access

Technical Note: Weight approximation of single coccoliths inferred from retardation estimates using a light microscope equipped with a circular polariser – (the CPR Method)

J. Bollmann

Department of Earth Sciences, Earth Sciences Centre, University of Toronto, 22 Russell Street, Toronto, Ontario, M5S 3B1, Canada

Received: 25 June 2013 – Accepted: 27 June 2013 – Published: 8 July 2013

Correspondence to: J. Bollmann (bollmann@es.utoronto.ca)

Published by Copernicus Publications on behalf of the European Geosciences Union.

Abstract

A new method for weight estimates of single coccoliths using the birefringence of calcite is described. The weight estimates of 364 Holocene coccoliths using this new method are in good agreement with published volumetric estimates. A robust calibration method based on the measurement of a calibration target of known retardation enables the comparison of data between different imaging systems. Therefore, the new method overcomes the shortcomings of the error prone empirical calibration procedure of a previously reported method based on birefringence of calcite. In addition, the new method includes the application of a circular polariser that eliminates the extinction pattern in crossed polarised light. This imaging method allows for the first time the imaging of complete coccoliths on a light microscope at maximum interference colours without moving any mechanical part of the microscope. Therefore, it greatly simplifies the identification of coccolithophore species on the light microscope as well as the calculation of the area and thus weight of a coccolith.

1 Introduction

Coccolithophores play a major role in the global carbon cycle and there are concerns that increasing ocean acidification affects the calcification of this group of phytoplankton (e.g. Doney et al., 2009). However, in order to quantify potential effects of ocean acidification on the calcium carbonate production of coccolithophores as a group or on the calcification of individual species, accurate estimates are required. Methods to quantify the carbonate weight of coccolithophores ranges from simple weighing the fine fraction of a sediment sample (e.g., $< 32\,\mu m$) (Broerse et al., 2000), weighing the samples before and after dissolving the carbonate (Bairbakhish et al., 1999), to elaborated morphometric measurements to estimate the weight of single coccoliths (Young and Ziveri, 2000; Beaufort and Heussner, 1999). A detailed review of the pros and cons of these methods is given in Beaufort (2005).

BGD
10, 11155–11179, 2013

Recently, efficient quantification methods were described based on the optical properties of calcite (birefringence). Guay and Bishop (2002) were first to report a method to quantify the bulk carbonate content of plankton samples using birefringence of particles in suspension with a benchtop spectrophotometer. However, the proposed method only allows for the quantification of bulk carbonate content and not the analysis of single coccoliths. Beaufort (2005) described a method that allows for the quantification of the weight of single coccoliths based on the optical properties of calcite and several studies have been utilising this new method (Beaufort et al., 2007, 2008, 2011; Grelaud et al., 2009; Cubillos et al., 2012; Bordiga et al., 2012). However, the transfer function reported by Beaufort (2005) is based on an error prone calibration method and suboptimal segmentation of coccoliths in crossed polarised light. Here, a new method is proposed that overcomes most of the limitations of the method reported by Beaufort (2005).

2 Material and methods

2.1 Conventions

The standard grey value scale is used here where black is 0 and white is 255 (8 bit grey scale). Pixel resolution refers to the size of a pixel and not to the optical resolution of the microscope. Please note that the pixel resolution changes with different imaging set-ups such as CCD chip size and optical resolution of the microscope (for details see Sect. 4.2).

2.2 Theoretical background

Birefringence of a mineral can be used to calculate the thickness of a particle if the particle is observed in Crossed Polarised Light (XPL) and Circular Polarised Light (CPL). In XPL/CPL the colour (interference colour) of a particle systematically changes with the thickness of the particle. The interference colours are the result of the difference of

BGD
10, 11155–11179, 2013

the index of refraction of the slow ray (ns) and that of the fast ray (nf) in a birefringent crystal. This difference increases with increasing thickness of the crystal and is called retardation (r = ns – nf, measured in nm). Zero nm retardation corresponds to black and for first order interference colours a retardation of 0–550 nm corresponds to black, grey, white, yellow and red (see Fig. 1a). If retardation and birefringence are known, the thickness and thus weight of a particle (e.g., a coccolith) can be calculated as follows:

$$t = r \times \frac{b}{1000} \quad (1)$$

where t = thickness (µm), r = retardation in nm, b = birefringence (0.172 for calcite)

Thus the weight can be calculated as follows:

$$w = a \times t \times d \quad (2)$$

where w = weight; a = surface area; t = thickness; d = density (2.71 for calcite).

In order to obtain the correct thickness of a particle, the highest interference colour/retardation of a particle has to be determined. This is achieved by rotating the particle under XPL until it shows the highest interference colour. The colour is then compared with colours shown on the Michel-Levy colour chart. This is a simple standard method for the analysis of minerals. There are, however, several more accurate but also more elaborate ways such as the Brace-Köhler analysis and the Senarmont compensator method to measure the retardation and thickness of birefringent material (Bloss, 1961; Zhang et al., 2013).

The Michel-Levy chart has been recently revised by Sørensen (2012) and therefore, it has been used in this study instead of the widely used charts of Zeiss or Leica. The new chart provides an improved representation of the interference colours and the calculation of interference colours was done in 1 nm steps retardation (Sørensen, 2012).

Please note that only the basic information is given here that is required to understand the method of weight calculation using birefringence of calcite crystals. A detailed

BGD
10, 11155–11179, 2013

explanation of the optical properties of unisotropic minerals and their analysis is beyond the scope of this study (for details, see Raith et al., 2012).

2.3 Imaging

All images were taken with a Zeiss Axio Imager Z1 equipped with a circular polarizer, a Plan-Apo 100×, 1.4 NA oil objective, 0.9 NA universal condenser, 1.6× optovar, and a Canon D60 DSLR camera. The camera resolution was set to 1920 × 1280 resulting in a pixel resolution of 0.002024523 μm^2. Please note that the pixel resolution is not the resolving power of the microscope (for details see Sect. 4.2). A micrometer scale with 10 µm divisions was used for size calibration (S8 Stage micrometer (02A00404) from PYSER-SGI LTD; overall accuracy < 0.0015 mm).

2.4 Illumination and retardation calibration

The illumination of the microscope was set to a constant colour temperature of 3200 K. The field aperture diaphragm of the microscope and shutter time as well as the film sensitivity of the camera and white balance were adjusted to match the interference colour/grey value of a quarter wave platelet a (140 nm ± 3 nm retardation; grey value = 194; see Supplement 1).

2.5 Image analysis

For image analysis (particle detection) and volume calculation, the programs ImageJ and AnalySIS 5 PRO, Olympus were used. Volume and weight calculations were done as follows: RGB images were converted into 8 bit grey scale images and the threshold for image segmentation and particle detection was set (background ~ 10 grey values). The [*calibration*] function of ImageJ was used to link grey values to weight per grey value (grey value = thickness × 2.71 (calcite density)) and a 4th degree polynomial function was used to fit the data calculated from the interference colours in 1 nm step retardation (Sørensen, 2012). The weight of a particle was calculated using the

BGD
10, 11155–11179, 2013

[*Analyze Particle...*] function of ImageJ where the weight of a particle is shown as [*Integrated Density*] (for details see http://rsbweb.nih.gov/ij/). The weight is the sum of all pixel values of one particle/coccolith.

2.6 Microscope slide preparation

Sediment suspensions were sprayed onto a glass slide to provide isolated particles that can be easily segmented (Bollmann et al., 1999, 2004; McIntyre et al., 1967) and subsequently a cover slip was mounted on the slide using Canada balsam. One Holocene sample (GEOB3602, 0–1 cm, Lat. 34°47.4′ S Long. 17°45.3′ E, 1885 m water depth) and one Late Pleistocene sample (DSDP 119-1-1, 31 cm, Lat. 45°01.90′ N, Long. 7°58.49′ W, water depth: 4447 m) were used.

3 Results

The conversion of interference colours of the latest colour chart by Sørensen (2012) into grey values shows that grey values increase approximately linear from black to white (retardation 0 – ~ 236 nm (Fig. 1)). 236 nm retardation corresponds to a maximum grey value of 253 (~white; Fig. 1b, c) and to a thickness of a calcite crystal of about 1.37 µm. Particles with a thickness from 1.37 µm (236 nm) to 1.45 µm have the same grey value of 253 (249 nm = average thickness of 1.41 µm). A regression analysis of the relationship between grey values and calcite thickness up to 1.41 µm revealed an R^2 of 0.99 for a 4th degree polynomial function. Therefore the weight of calcite (thickness × calcite density; 2.71) per grey value can be estimated using the following formula:

$$Y = a + bx + cx^2 + dx^3 + ex^4 \quad (3)$$

where Y = weight; x = grey value; a = 0.0713749; b = 0.00312707; c = 0.000145114; $d = -1.012611 \times 10^{-6}$; $e = 2.415926 \times 10^{-9}$.

If the area of a particle and the corresponding number of pixels is known, the total weight of the particle is the sum of all grey values/weights of all pixels (see Sect. 2.5).

BGD
10, 11155–11179, 2013

However, the area of a coccolith in XPL is not easily calculated. The optical axis of coccolith crystal units is often oblique to the optical axis of the microscope and arranged in a radial pattern (for details see Young and Bown, 1997). Therefore, parts of a coccolith appear dark in XPL (extinction pattern) and can not be separated from the dark background.

To overcome this fundamental problem of calculating the area of a coccolith in XPL, a circular polarizer was used in this study (Benford plate; Craig, 1961). This simple device eliminates the extinction pattern caused by the crossed polarising filters and coccoliths exhibit their highest interference colours independent of their orientation with respect to the polarizer and analyser. There is no need to rotate the coccolith to find the highest interference colour. Thus the CPL method eliminates a major source of error and uncertainty for the weight estimates and it significantly simplifies the identification of coccolithophore species (Fig. 5a–p). The weight difference using the outline/area in XPL and CPL is about 45 %, for example for the specimen of *Gephyrocapsa oceanica* shown in Fig. 5c, q: XPL 10pg, r: CPL 18pg).

About 360 single coccoliths of 16 Holocene coccolithophore taxa were analysed using the new weight transfer function in combination with the new imaging technique (Table 1; Supplement 2). Weight estimates are well within the range of published values for coccoliths of the family Noelaerhabdaceae and coccoliths of Incertae Sedis taxa Umbellosphaeraceae and *Florisphaera* (Fig. 2a-f, Fig. 5a-f). Furthermore, the weight of coccoliths of *Rhabdosphaera* sp. can be estimated up to a length of about 9.5 µm. Larger specimens exhibit yellow interference colours and are therefore outside of the calibration range (Fig. 2g, Fig. 5g). In contrast, the weight of coccoliths of the order Zygodiscales, Coccolithales and the family Syracosphaeraceae (Fig. 2i–p) can not be simply calculated using birefringence because the C-axis orientation of some crystal units has been reported to be parallel to the optical axis of the microscope and thus appear to be dark in XPL/CPL (V-units according to Young and Bown, 1997). For example, the distal shield of *Coccolithus pelagicus*, *Calcidiscus leptoporus* and *Umbilicosphaera* spp. is expected to be dark in XPL/CPL and therefore should not be distinguishable

BGD
10, 11155–11179, 2013

from the dark background. Consequently, the new method underestimates the weights of coccoliths of these taxa systematically in comparison to weights estimates based on volumetric estimates (Young and Ziveri, 2000; Beaufort and Heussner, 1999) (Fig. 2i-n). Furthermore, coccoliths of *C. pelagicus, Helicosphaera* sp. and *C. leptoporus* larger than ~ 8 µm show yellow-reddish interference colours indicating that their thickness is beyond the calibration range of 1.41 µm thickness (Fig. 2i, j, m; Fig. 5i, j, m).

4 Discussion

The good agreement between weight estimates based on volumetric weight estimates (Young and Ziveri, 2000) and the new method (Fig. 2a–c, e–f) validates the applicability of the new method for weight estimates of coccoliths of the family Noelaerhabdaceae and coccoliths of Incertae Sedis taxa Umbellosphaeracea. However, the weight estimates for *F. profunda* differ significantly (Fig. 2d). The weight estimates of *F. profunda* coccoliths do not increase with increasing length as expected (Young and Ziveri, 2000) and as observed for most other species such as *G. oceanica* (Fig. 3). One possible explanation for the difference is that the three different morphotypes/varieties of *F. profunda* (Quinn et al., 2005) have different shape factors (K_s values) or do not follow the formula:

$$\text{Volume} = K_s \times (\text{Length})^3 \quad (4)$$

where K_s is the species specific shape factor (Young and Ziveri, 2000).

Also, the relatively large scatter of weight estimates for *E. huxleyi*/small placoliths (Fig. 2a) might be explained by the presence of different morphotypes and species, as well as varying degrees of preservation. *E. huxleyi* comprises several morphotypes with different K_s values (Young and Ziveri, 2000) that can not be separated using a light microscope. Furthermore, most coccoliths smaller than ~ 3 µm can not be unequivocally recognised as *E. huxleyi, Gephyrocapsa* spp. or *Reticulofenestra* spp. using a

BGD
10, 11155–11179, 2013

light microscope. All of these taxa have different K_s values that might contribute to the scatter in Fig. 2a.

Most weight estimates reported by Beaufort (2005) appear to be higher than the values reported here even if the maximum coccolith length for a given species is assumed (Fig. 2). This is surprising as the method is also based on birefringence of calcite. One possible explanation for the discrepancies is the calibration method used by Beaufort (2005). Beaufort (2005) also utilised the fact that the interference colour transformed into grey values is proportional to the thickness of a mineral to estimate the weight of calcite particles. However, the calibration of the weight transfer function relates known sample weights of calcite particles to average grey values in a field of view (Fig. 4). This approach leads to inaccurate weight estimates because not all particles show their maximum interference colour/grey value as they are randomly distributed with respect to the Crossed Polariser (XPL). Furthermore, the orientation of a crystal/particle strongly depends on its habitus. Particles might have preferred orientations depending on the habitus. Some of the particles might even be black if the C-axis orientation is parallel to the optical axis of the microscope. This biases the results towards heavier weights/pixel with respect to the average interference colour/grey value in a frame of view and the use of different material (different particle shapes and sizes) for calibration results in numerous different calibration curves.

Another shortcoming of the calibration method by Beaufort (2005) is the use of particles that are outside the valid range of 0 – 1.56 µm thickness (please note that a maximum particle thickness of 1.56 µm was given by Beaufort, 2005). From Fig. 1 it is evident that particles with different thicknesses can have the same grey value representation. For example, a pixel with a grey value of 100 can correspond to a thickness/weight of 2.9 µm/0.176 pg; 3.4 µm/0.206 pg or just 0.38 µm/0.023 pg (Fig. 1). However, Beaufort (2005) used particles from 1 to 5 µm to calibrate and establish a transfer function for calculating the weight per pixel from grey values. Consequently the transfer function significantly overestimates the weight per pixel in comparison to the calibration reported here (Fig. 4). The maximum weight per pixel using the weight transfer func-

BGD
10, 11155–11179, 2013

tion by Beaufort (2005) is 0.196 pg (~ 196 grey value level/1000; red checker board in Fig. 4). This is about double the weight based on the maximum particle size of 1.56 µm valid to be used (Beaufort, 2005).

The use of particles outside the valid range (larger than 1.56 µm as reported by Beaufort, 2005) for calibration and the fact that the grey value of a particle depends on its orientation in XPL explain why the transfer function reported by Beaufort (2005) spans only grey values up to a maximum grey value of 110 (Fig. 4) and why it significantly overestimates the weight per pixel. Considering these facts, the empirical calibration first reported by Beaufort (2005) and all subsequent derivatives (Beaufort et al., 2007, 2008, 2011; Cubillos et al., 2012) are not suitable to accurately calculate coccolith and coccosphere weights and thus lead to biased results and potentially invalid interpretations.

4.1 Limitations of the presented method

The weight of coccoliths with the C-axis of their crystal units oriented parallel to the optical axis of the microscope can not be accurately estimated as they appear to be isotropic (dark in XPL; V-units according to Young and Bown (1997); e.g., discoasterids, coccoliths of the order Zygodiscales, Coccolithales and the family Syracosphaeraceae, Fig. 2i–p). Surprisingly the new method provides a good approximation of coccolith weights of *C. leptoporus*, *Helicosphaera* and *Umbilicosphaera* compared to the volumetric approach by Young and Ziveri (2000) if the thickness does not exceed the calibration range of 1.41 µm thickness (large specimens). A possible explanation for the good agreement with volumetric estimates is that the V-units are not exactly oriented parallel to the optical axis of the microscope. This might be the case if coccoliths are not lying flat on the slide or if the orientation of the V-units within a coccolith is not exactly vertical. Furthermore, particles thinner than 0.04 µm can not be measured as they can not be separated from the background (~ grey value of 10 in this study; this limitation depends on the quality of the optics of the microscope and their alignment). The most significant limitation of the method is the restriction to particles thinner than

BGD
10, 11155–11179, 2013

~ 1.41 µm. This limits the application of the method to the analysis mainly of single coccoliths. The accurate calculation of the weight of coccospheres using birefringence as reported by Beaufort et al. (2011, 2008) appears to be challenging as the stacked thickness of coccoliths on a coccosphere can easily exceed 1.41 µm. The stacked thickness of a side view of a single coccolith, for example an *E. huxleyi* coccolith with a length of 2.5 to 3.5 µm, exceeds clearly the limits of the applicability of a method based on weight estimates using the relationship between grey values derived from interference colours.

4.2 Error considerations

There are three main sources of error.

1. Resolution of retardation and weight estimates
2. Spatial resolution of the microscope
3. Dispersion colours

4.2.1 Accuracy of retardation calculation and weight estimates

For calibration, a quarter wave plate of 140 nm ± 3 nm revealed a grey value of 193 ± 1 stdev. The corresponding grey value for a retardation of 140 nm is 194 according to the conversion of interference colours into grey values. In order to test the accuracy of the calibration, the interference colour of a birefringent polymer with a retardation of 165 ± 3 nm was measured and revealed a grey value of 218 ± 1 stdev. The corresponding grey value based on the conversion of interference colours into grey values for a retardation of 165 nm is 217. The smallest difference in thickness and weight that can be resolved is on average about 0.005 µm and 0.013 pg of calcite up to a grey value of 250. From 251 to 253 one grey value corresponds to 0.16 pg of calcite.

BGD
10, 11155–11179, 2013

4.2.2 Spatial resolution of the microscope

The overall resolution of the method also depends on the spatial resolution of the microscope. The theoretical spatial resolution of a microscope is determined by the numerical aperture of the objective (NA of 1.4 in this study) and the condenser (NA of 0.9 this study) and the wavelength of the light source (here 550 nm) and is calculated as follows:

$$\text{ors} = \frac{1.22 \times \lambda}{\text{NA}_{\text{obj}} + \text{NA}_{\text{cond}}} \quad (5)$$

where ors = optical resolution; λ = wavelength of the light used; NA_{obj} = numerical aperture of the objective; NA_{cond} = numerical aperture of the condenser.

For the setup used in this study the theoretical resolution is 0.291 µm. However, a realistic practical resolution is about 0.5 µm for the system used and all dimensional measurements have a minimum error of ±0.25 µm. Considering the optical resolution and the resolution of thickness calculation, the resolution of the total weight estimation can be approximated as follows:

$$w = a \times t_{\text{m}} \times d \quad (6)$$

where w = coccolith weight; a = coccolith area; d = density (here 2.71 for calcite); t_{m} = mean thickness;

$$t_{\text{m}} = t_{\text{m}} \pm \frac{t_{\text{rs}}}{2} \quad (7)$$

where t_{rs} = thickness resolution (0.005 µm this study)

$$a = \text{ael} - \text{caa} \quad (8)$$

BGD
10, 11155–11179, 2013

where ael = area of an ellipse fit using length and width of the coccolith; caa = area of an ellipse fit using the length (cal) and width (caw) of the central area.

$$\text{ael} = \pi \times \left(\frac{\left(\text{cl} \pm \frac{\text{ors}}{2}\right)}{2} \right) \times \left(\frac{\left(\text{cw} \pm \frac{\text{ors}}{2}\right)}{2} \right) \quad (9)$$

where cl = coccolith length; cw = coccolith width; ors = optical resolution (0.291 µm this study);

$$\text{caa} = \pi \times \left(\frac{\left(\text{cal} \pm \frac{\text{ors}}{2}\right)}{2} \right) \times \left(\frac{\left(\text{caw} \pm \frac{\text{ors}}{2}\right)}{2} \right) \quad (10)$$

where cal = length of central area; caw = width of the central area.

Using the above listed approach the weight resolution can only be approximated as it assumes perfect ellipses. Furthermore, special elements, for example, the bridge element spanning the central area of *Gephyrocapsa* spp. are not taken into account. The resolution of the weight estimate for *G. oceanica* given on Fig. 5r is ~ ±2.16 pg (±12 % of 18 pg). If an optical resolution of 0.5 µm is assumed, the resolution of the weight estimate deteriorates to ±3.6 pg (±20 % of 18 pg).

4.2.3 Dispersion colours

Blue dispersion colours were often observed at the edge of coccoliths in XPL and CPL (Fig. 5) that can lead to erroneous weight calculations. Accurate focussing and adjusting of the threshold for object detection reduces the error but it does not eliminate the error. Different mounting media (different refractive index than Canada balsam) might reduce the problem as the phenomenon appears to be caused by differences in refractive index of the mounting medium and calcite resulting in a coloured Becke line.

BGD
10, 11155–11179, 2013

4.3 Recommendation

1. It is recommended to restrict the weight estimates to a coccolith thickness of 1.27 µm and the corresponding grey value of 250 because the resolution of the method declines significantly from 0.013 pg to 0.16 pg for grey values higher than 250. This can be done in ImageJ by setting an upper threshold for the segmentation/detection of particles.

2. As higher interference colours of thicker particles can show the same grey value, it is recommended to use a colour camera and remove all particles that show colours higher than first order white before the image is transformed into a grey scale image. Once an image is converted into a grey scale image this filtering is not possible anymore. It should be noted that great care has to be taken when RGB colours are converted into grey values because there are different algorithms resulting in different results (ditto for black and white cameras). It is best to use the same Imaging program to convert the Michel-Levy chart and the microscope images into grey scale images to avoid calculation bias.

3. If membrane filters are used for the preparation, it should be tested whether the membranes are birefringent. For example, polycarbonate membranes are birefringent and affect the measurements as they can lower or increase the interference colour of calcite particles.

4. If the mean coccolith weight of a species has to be compared from several samples, it is suggested to conduct first a pilot study to get an idea of the expected standard deviation of the samples to be measured. The number of coccoliths per sample to be measured can then be calculated by:

$$n = \frac{z^2 \times o^2}{\mathrm{er}^2} \tag{11}$$

BGD
10, 11155–11179, 2013

where n = number of specimens; er = Tolerable error ± from the mean value; σ expected standard deviation; z = critical standard score, e.g. 1.96 for a 95 % confidence interval.

For example, the mean weight of *G. muellerae* in GEOB3602 is 7.6 pg and the 95 % confidence interval for the mean value is ±1.3 pg (standard deviation is ±2.7 pg). If the tolerable error for the mean value has to be smaller than 1.3 pg, for example, 1.0 pg (~ weight resolution of the new method), the number of measurements has to be increased from 16 to 28 measurements. The same approach can be used to determine the number of measurements required for any dimensional measurement (for details see http://stattrek.com/sample-size/simple-random-sample.aspx).

5. It is recommend to use the spraying method reported by Bollmann et al. (1999) and McIntyre et al. (1967) to prepare sediment samples instead of using the generic smear slide method as it provides well isolated coccoliths for a robust segmentation of coccoliths and outline detection.

6. Vibrations can significantly reduce the spatial resolution of the microscope and thus increase the error on weight estimates. Therefore the use of an anti-vibration table or table top is recommended.

4.4 Useful online resources

http://www.modernmicroscopy.com/
http://micro.magnet.fsu.edu
http://www.olympusmicro.com/index.html
http://www.microscopyu.com/
http://zeiss-campus.magnet.fsu.edu/
http://stattrek.com/sample-size/simple-random-sample.aspx

BGD
10, 11155–11179, 2013

5 Conclusions

The proposed method overcomes most limitations of the weight transfer function proposed by Beaufort (2005) as it is derived from theoretical considerations instead of error prone empirical calibrations. The simple calibration of the interference colour/grey level using a material with a known thickness/retardation and birefringence has several advantages. It is quick and can be done just before the actual batch of measurements. A bias due to aging light bulbs and varying illumination between batches does not affect the result. The accuracy of the calibration can be tested by measuring the grey values of material with known retardation different from the one used for calibration. It also provides the simple means to compare the results from different studies as standard retardation wave plates can be used to calibrate the interference colours on different systems. Furthermore, the use of the Benford plate overcomes the problem of extinction patterns in XPL and thus increases the accuracy of the weight estimates. This new imaging technique enables for the first time the imaging of complete coccoliths with maximum interference colour and therefore, it greatly simplifies the identification of coccolithophore species on a light microscope.

Supplementary material related to this article is available online at: http://www.biogeosciences-discuss.net/10/11155/2013/bgd-10-11155-2013-supplement.pdf.

Acknowledgements. Bjørn Eske Sørensen kindly provided his new colour chart in a resolution of 1 nm steps retardation. This work would not have been possible without continuous support from Manuel Schneidereith, Customized Solutions, Olympus Soft Imaging Solutions GmbH. Comments from Jens Olaf Herrle and Mara Yadira Cortés helped to improve the ms.

References

Bairbakhish, A. N., Bollmann, J., Sprengel, C., and Thierstein, H. R.: Disintegration of aggregates and coccospheres in sediment trap samples, Mar. Micropaleontol., 37, 219–223, 1999.

Beaufort, L.: Weight estimates of coccoliths using the optical properties (birefringence) of calcite, Micropaleontology, 51, 289–298, 2005.

Beaufort, L. and Heussner, S.: Coccolithophorids on the continental slope of the Bay of Biscay – production, transport and contribution to mass fluxes, Deep-Sea Res. Pt. II, 46, 2147–2174, 1999.

Beaufort, L., Probert, I., and Buchet, N.: Effects of acidification and primary production on coccolith weight: Implications for carbonate transfer from the surface to the deep ocean, Geochem. Geophys. Geosyst., 8, 1–18, doi:10.1029/2006GC001493, 2007.

Beaufort, L., Couapel, M., Buchet, N., Claustre, H., and Goyet, C.: Calcite production by coccolithophores in the south east Pacific Ocean, Biogeosciences, 5, 1101–1117, doi:10.5194/bg-5-1101-2008, 2008.

Beaufort, L., Probert, I., de Garidel-Thoron, T., Bendif, E. M., Ruiz-Pino, D., Metzl, N., Goyet, C., Buchet, N., Coupel, P., Grelaud, M., Rost, B., Rickaby, R. E. M., and de Vargas, C.: Sensitivity of coccolithophores to carbonate chemistry and ocean acidification, Nature, 476, 80–83, 2011.

Bloss, F. D.: An Introduction to the Methods of Optical Crystallography Holt, Philadelphia, Pa., 1961.

Bollmann, J.: Morphology and biogeography of *Gephyrocapsa* coccoliths in Holocene sediments, Mar. Micropaleontol., 29, 319–350, 1997.

Bollmann, J., Herrle, J. O.: Morphological variation of Emiliania huxleyi and sea surface salinity, Earth Planet. Sc. Lett., 255, 273–288, 2007.

Bollmann, J., Brabec, B., Cortes, M. Y., and Geisen, M.: Determination of absolute coccolith abundances in deep-sea sediments by spiking with microbeads and spraying (SMS-method), Mar. Micropaleontol., 38, 29–38, 1999.

Bollmann, J., Quinn, P., Vela, M., Brabec, B., Brechner, S., Cortés, M. Y., Hilbrecht, H., Schmidt, D. N., Schiebel, R., and Thierstein, H. R.: Automated particle analysis: calcareous microfossils., Image Analysis, Sediments and Paleoenvironments, edited by Francus, P., Springer, Berlin, New York, 229–252, 2004.

BGD
10, 11155–11179, 2013

Bollmann, J., Klaas, C., and Brand, L. E.: Morphological and physiological characteristics of *Gephyrocapsa oceanica* var. typica Kamptner 1943 in culture experiments: evidence for genotypic variability, Protist, 161, 78–90, doi:10.1016/j.protis.2009.08.002, 2010.

Bordiga, M., Beaufort, L., Cobianchi, M., Lupi, C., Mancin, N., Luciani, V., Pelosi, N., and Sprovieri, M.: Calcareous plankton and geochemistry from the ODP site 1209B in the NW Pacific Ocean (Shatsky Rise): new data to interpret calcite dissolution and paleoproductivity changes of the last 450ka, Palaeogeogr. Palaeocl., 371, 93–108, 2012.

Broerse, A. T. C., Brummer, G. A., and Hinte, J. E. V.: Coccolithophore export production in response to monsoonal upwelling off Somalia (northwestern Indian Ocean), Deep-Sea Res. Pt. II, 47, 2179–2205, 2000.

Cubillos, J. C., Henderiks, J., Beaufort, L., Howard, W. R., and Hallegraeff, G. M.: Reconstructing calcification in ancient coccolithophores: Individual coccolith weight and morphology of *Coccolithus pelagicus* (sensu lato), Mar. Micropaleontol., 92–93, 29–39, 2012.

Doney, S. C., Fabry, V. J., Feely, R. A., and Kleypas, J. A.: Ocean Acidification: The other CO_2 problem, Annu. Rev. Mar. Sci., 1, 169–192, 2009.

Grelaud, M., Schimmelmann, A., and Beaufort, L.: Coccolithophore response to climate and surface hydrography in Santa Barbara Basin, California, AD 1917–2004, Biogeosciences, 6, 2025–2039, doi:10.5194/bg-6-2025-2009, 2009.

Guay, C. K. H. and Bishop, J. K. B.: A rapid birefringence method for measuring suspended $CaCO_3$ concentrations in seawater, Deep-Sea Res. I, 49, 197–210, 2002.

Knappertsbusch, M., Cortes, M. Y., and Thierstein, H. R.: Morphologic variability of the coccolithophorid *Calcidiscus leptoporus* in the plankton, surface sediments and from the Early Pleistocene, Mar. Micropaleontol., 30, 293–317, 1997.

McIntyre, A., Bé, A. W. H., and Preikstas, R.: Coccoliths and the Pliocene-Pleistocene boundary, Prog. Oceanogr., 4, 3–25, 1967.

Parente, A., Cachão, M., Baumann, K.-H., Abreu, L. D., and Ferreira, J.: Morphometry of *Coccolithus pelagicus* s.l. (Coccolithophore, Haptophyta) from offshore Portugal, during the last 200 kyr, 50, 107–120, 2004.

Quinn, P. S., Cortes, M. Y., and Bollmann, J.: Morphological variation in the deep ocean-dwelling coccolithophore *Florisphaera profunda* (Haptophyta), Eur. J. Phycol., 40, 123–133, 2005.

Raith, M. M., Raase, P., and Reinhardt, J.: Guide to Thin Section Microscopy, 2nd Edn., 2012.

Sørensen, B. E.: A revised Michel-Lévy interference colour chart based on first-principles calculations, Eur. J. Mineral., 25, 5–10, 2012.

BGD
10, 11155–11179, 2013

Young, J. R. and Bown, P. R.: Higher classification of calcareous nannofossils, J. Nannoplankton Res., 19, 15–20, 1997.
Young, J. R., and Ziveri, P.: Calculation of coccolith volume and its use in calibration of carbonate flux estimates, Deep-Sea Res. Pt. II, 47, 1679–1700, 2000.
Zhang, P., Tan, Y., Liu, W., and Chen, W.: Methods for optical phase retardation measurement: a review, Sci. China Technol. Sci., 56, 1155–1164, doi:10.1007/s11431-013-5207-4, 2013.

BGD
10, 11155–11179, 2013

Table 1. Comparison of published weight estimates. *N* = Number of measurements; STDEV = Standard deviation of weight estimates reported; K_s = shape factor reported by Young and Ziveri (2000). Values for maximum length of single coccoliths for *E. huxleyi* were reported by Bollmann and Herrle (2007), for *Gephyrocapsa* spp. by Bollmann (1997) and Bollmann et al. (2010), for *F. profunda* by Quinn et al. (2005), for *C. leptoporus* by Knappertsbusch et al. (1997), for *C. pelagicus* by Parente et al. (2004). Values for all other species were taken from Young and Ziveri (2000). Please note that the average length for populations are significantly smaller, for example, for *E. huxleyi* the maximum average length of a Holocene sample is smaller than 4 µm although the maximum size of a single coccolith can be up to 6 µm (Bollmann and Herrle, 2007).

	Taxa	*N*	Average weight (pg) This study	STDEV	Length (µm)	Weight (pg) Beaufort (2005)	Weight (pg) Beaufort and Heussner (1999)	Length (µm)	Max. K_s Weight (pg) Young and Ziveri (2000)	Min. K_s Weight (pg) Young and Ziveri (2000)	Min. K_s Value Young and Ziveri (2000)	Max. K_s Value Young and Ziveri (2000)	Max. Length/K_s weight (pg)	Max. Length (µm)
A	Small placoliths/*E. huxleyi*	70	1.7	0.9	2.5	5.3	2.9	3.10	1.7	0.6	0.014	0.040	23.4	6.0
B	*G. muellerae*	22	7.0	2.7	3.6	–	25.7	5.35	6.3	6.3	0.050	0.050	16.9	5.0
C	*G. oceanica*	29	14.5	8.0	4.3	53	–	–	12.9	8.0	0.037	0.060	35.1	6.0
D	*F. profunda*	57	1.0	0.6	2.6	2.2	6.8	4.20	2.9	1.4	0.030	0.060	99.9	8.5
E	*U. tenuis*	13	8.4	2.7	5.6	–	23.9	5.00	7.6	5.7	0.012	0.016	22.2	8.0
F	*U. irregularis*	3	7.7	3.3	7.8	–	–	–	12.9	12.9	0.010	0.010	13.9	8.0
G	*Rhabdosphaera* spp.	23	11.7	7.6	8.3	46	–	–	40.3	17.0	0.011	0.026	121.8	12.0
H	*Calciosolenia* spp.	10	2.5	1.8	5	–	–	–	–	–	–	–	–	–
I	*C. leptoporus*	35	30.0	19.0	6	109	125.0	8.10	60.3	39.8	0.068	0.103	686.8	13.5
J	*H. carteri*	36	57.1	23.0	9.1	142	143.0	9.11	102.1	102.1	0.050	0.050	234.1	12.0
K	*S. pulchra*/*Syracosphaera* spp.	14	5.9	2.7	5.4	10–22	17.0	5.85	14.1	6.4	0.015	0.033	30.7	7.0
L	*U. sibogae*	30	7.0	6.1	4.1	18	16.0	4.10	15.7	8.0	0.043	0.084	49.2	6.0
M	*C. pelagicus*	8	111.3	37.2	10.3	–	151.2	10.35	207.3	118.5	0.040	0.070	520.5	14.0
N	*Ceratolithus* HET	10	5.8		6.7	–	–	–	13.0	12.2	0.015	0.016	43.4	10.0
N	*Ceratolithus* CER	1	31.2	3.1	6.9	–	–	–	89.0	86.4	0.097	0.100	360.7	11.0
O	*P. discopora*	1	65.0		7.2	–	–	7.90	–	–	–	–	–	–
O	*P. multipora*	2	30.0	10.0	7.2	–	–	–	–	–	–	–	–	–
P	*P. japonica*	1	45.0		7.7	–	70.1	8.20	–	–	–	–	–	–

BGD
10, 11155–11179, 2013

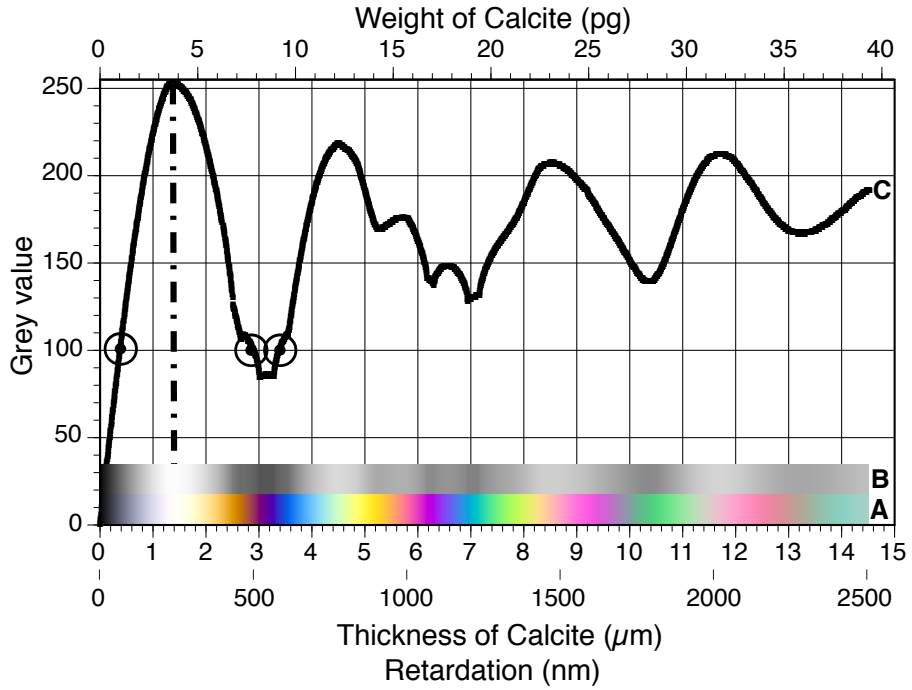

Fig. 1. Relationship between interference colour, retardation, thickness and weight of calcite. A Raith-Sørensen colour chart calculated in 1 nm steps retardation (Sørensen, 2012); B and C Conversion of the Raith-Sørensen colour chart (RGB) into grey values from 0–255 using ImageJ. The thickness and weight of calcite were calculated according to Eqs. (1) and (2), respectively. The dashed dotted line (–·–) indicates the boundary, beyond which, the weight of calcite can not be determined using the linear relationship between grey value and weight of a pixel. Marker (⊙) indicates the different thicknesses/weights for a grey value of 100 assuming a pixel area of 0.0225 µm^2: 2.9 µm, /0.177 pg; 3.4 µm/0.207 pg or just 0.38 µm/0.023 pg.

BGD
10, 11155–11179, 2013

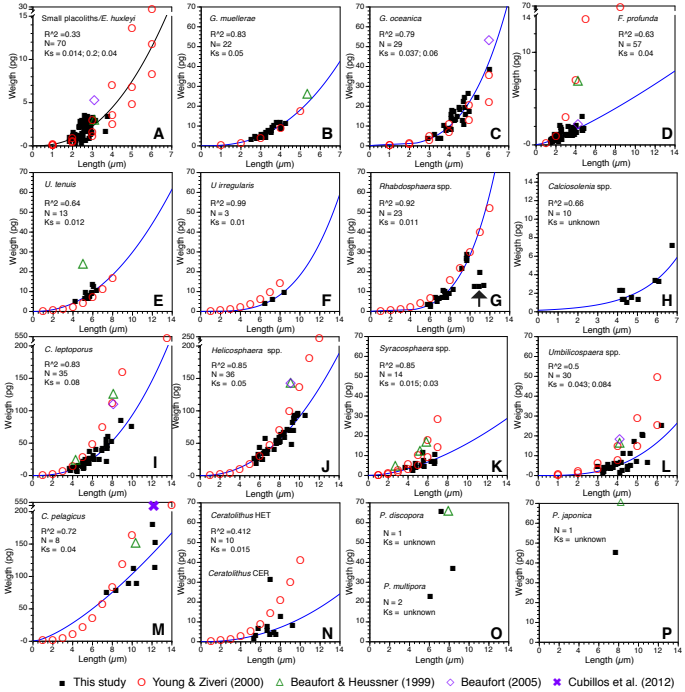

Fig. 2. Comparison between weight estimates of 16 Holocene coccolith taxa obtained with the new method and published values. K_s = shape factor introduced by Young and Ziveri (2000); the weight of a coccolith was calculated as follows: Weight = $K_s \times (\text{Length})^3 \times 2.71$ (density of calcite). Minimum and maximum K_s values given by Young and Ziveri (2000) were used to calculate the coccolith weights; Values for maximum length of coccoliths for *E. huxelyi* were reported by Bollmann and Herrle (2007), for *Gephyrocapsa* spp. by Bollmann (1997) and Bollmann et al. (2010), for *F. profunda* by Quinn et al. (2005), for *C. leptoporus* by Knappertsbusch et al. (1997), for *C. pelagicus* by Parente et al. (2004). Values for all other species were taken from Young and Ziveri (2000). R^2 = regression coefficient for the regression line. The arrow in **(G)** indicates *Rhabdosphaera* spp. larger than 9.5 µm.

BGD
10, 11155–11179, 2013

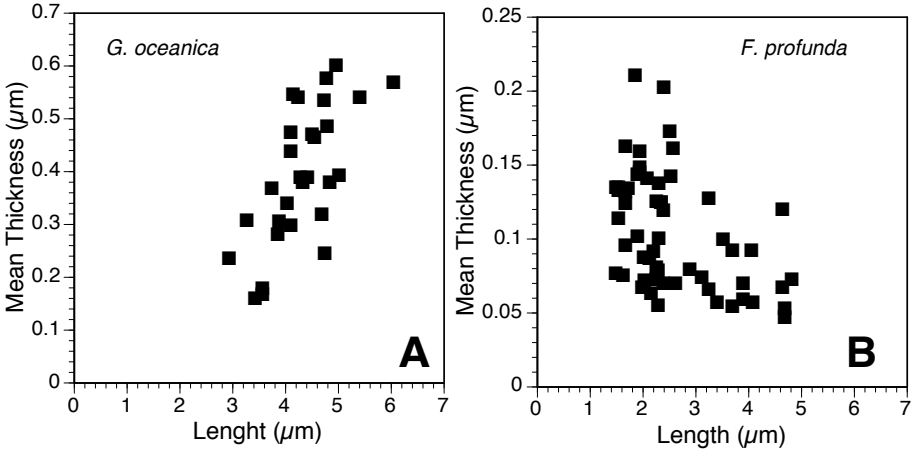

Fig. 3. Scatter plots of length versus thickness for *G. oceanica* **(A)** and *F. profunda* **(B)** indicating that the thickness of *F. profunda* does not increase with increasing length as it does in most other species.

BGD
10, 11155–11179, 2013

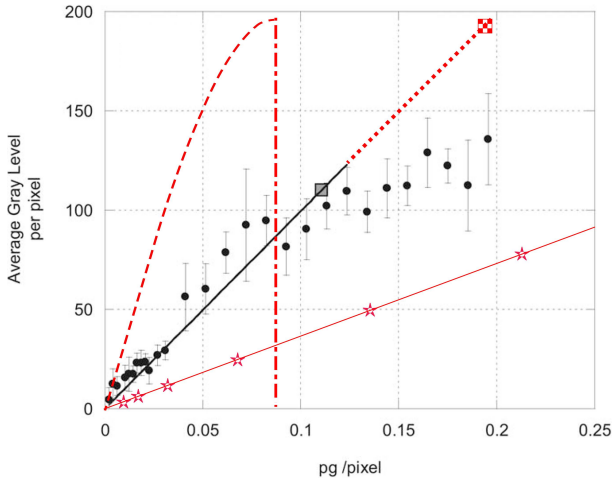

Fig. 4. Coccolith weight calibration reported by Beaufort (2005). Figure modified after Beaufort's (2005) Fig. 1A. Black/Grey indicates that the information is from Beaufort (2005) and Red indicates the data added here. Original caption by Beaufort (2005) Quote: "Relationship between the weight of calcite on the membrane per pixel unit (x axis) and the average gray level value per pixel in hundred fields of view with the 2 sigma standard deviation (y axis). The regression line is computed for weight below 0.125 pg/pixel and forced to go to the axis origin .... The grey square in A represents the expected position of a grain having the volume of pixel x 1.5 micrometer (change from white to yellow in Michel-Levy chart) divided by two in order to take into account the effect of the isogyre in the calibration". Red dashed line (- - -) indicates the relationship between grey values calculated from the Raith-Sørensen colour chart and weight per pixel inferred from thickness calculation based on retardation. This relationship was used in this study to estimate the weight of single coccoliths. – Note that the area of one pixel is 0.0225 μm^2 and that the grey values have been mapped into a grey value space from 0–196 to be comparable with the values published by Beaufort (2005). Solid red line with red open stars (☆) indicates a fictive calibration curve following the calibration approach of Beaufort (2005) using particles with a thickness of 3.4 µm corresponding to a grey value of 100 (see also marker in Fig. 1). Please note that the slope of calibration curves using the approach of Beaufort (2005) depends strongly on the shape and thickness of the particles used resulting in numerous different calibration curves (e.g., long prismatic versus short prismatic crystals have different preferred orientations with respect to XPL). Red dashed dotted line (- · -) indicates the boundary, beyond which, the weight of calcite can not be determined using the relationship between grey values and weight of a pixel as reported in this study (1.41 µm); Dashed red black line (▪▪▪▪) indicates the extrapolated weights using the transfer function by Beaufort (2005); Red checker board (✤) indicates the maximum theoretical weight per pixel using the transfer function pg = 196/996 by Beaufort (2005); 196 is the maximum grey level in Beaufort's study.

BGD
10, 11155–11179, 2013

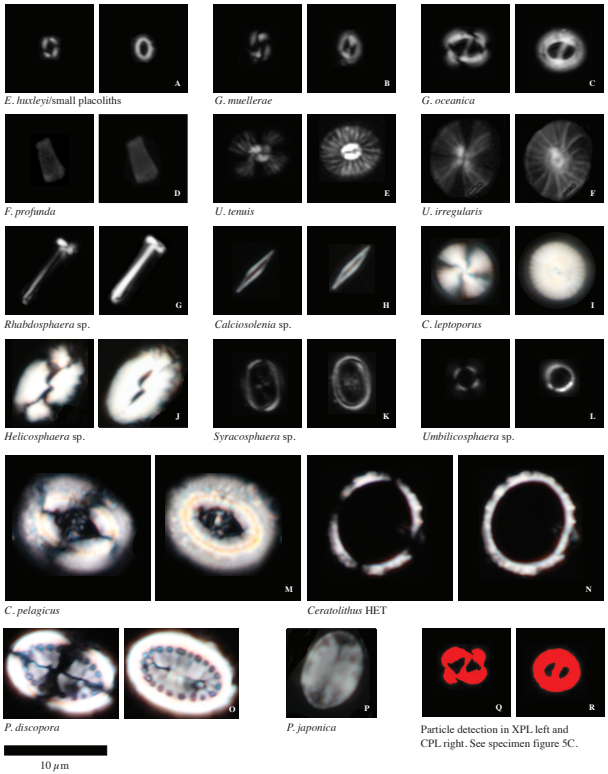

Fig. 5. Holocene coccoliths depicted in XPL and CPL. **(A–O)** show the same specimens in XPL (left image) and in CPL (right image). All images were taken with a ZEISS Axio Imager Z1 with an PlanApo. 1.4 NA, 100x oil objective, 0.9 NA universal condenser using a Canon 60D. **(Q)** and **(R)** show the difference in coccolith detection and resulting difference in weight estimates using XPL (10pg; **Q**) and CPL (18pg; **R**), respectively. Scale bar = 10 µm.

BGD
10, 11155–11179, 2013